CONFERENCE PRE-PRINT

STUDY OF FAST ION TRANSPORT AND LOSSES DURING ALFVÉN TYPE MHD INSTABILITIES AT GLOBUS-M2

O.M. SKREKEL, N.N. BAKHAREV, A.S. ALEXANDROV, I.M. BALACHENKOV, V.I. VARFOLOMEEV, A.V. VORONIN, V.K. GUSEV, N.S. ZHILTSOV, E.O. KISELEV, G.S. KURSKIEV, A.D. MELNIK, V.B. MINAEV, I.V. MIROSHNIKOV, A.N. NOVOKHATSKY, YU.V. PETROV, N.V. SAKHAROV, A.YU. TELNOVA, E.E. TKACHENKO, V.A. TOKAREV, E.A. TUKHMENEVA, E.M. KHILKEVICH, F.V. CHERNYSHEV, A.E. SHEVELEV, K.D. SHULYATIEV, P.B. SHCHEGOLEV, A.Y. YASHIN
Ioffe Institute
St. Petersburg, Russian Federation
Email: skrekel@mail.ioffe.ru

A.V. BONDAR, E.N. BONDARCHUK, A.A. KAVIN, I.V. KEDROV, A.B. MINEEV, V.N. TANCHUK, V.A. TROFIMOV, A.A. VORONOVA
JSC «NIIEFA»
St. Petersburg, Russian Federation

A.M. PONOMARENKO
Peter the Great St. Petersburg Polytechnic University
St. Petersburg, Russian Federation

A.N. KVASHNIN, E.I. PINZHENIN, A.D. KHILCHENKO
Budker Institute of Nuclear Physics
Novosibirsk, Russian Federation

A.S. DZHURIK, YU.A. KASHCHUK, S.YU. OBUDOVSKY
Project Center ITER
Moscow, Russian Federation

Abstract

A comprehensive study of TAE- and EPM-induced fast ion transport and losses at the Globus-M/M2 spherical tokamaks is presented. The results demonstrate that the dominant transport mechanism is convective resonant transport, leading to significant fast ion losses across a wide energy range. A key finding is the identification of two distinct components in the heat flux to the wall: a coherent part, synchronous with the mode and resulting from direct ion orbit losses, and an incoherent part, attributed to enhanced charge-exchange losses of ions transported to the plasma periphery. Both components exhibit a linear threshold-like dependence on the TAE amplitude. This dependence is successfully explained by a full-orbit Monte Carlo simulation. The model demonstrates that the instability must reach a critical amplitude to expel ions from the high-density plasma core. At lower amplitudes, wave-induced transport is limited to the low-density periphery, resulting in negligible losses. This behavior is consistent with a convective transport mechanism rather than with stochastic diffusion. Furthermore, initial investigations of EPMs provide direct experimental evidence of ion redistribution and loss caused by these instabilities at Globus-M2. The results underscore the critical impact of Alfvénic instabilities on fast ion confinement and wall power loads in spherical tokamaks.

1. INTRODUCTION

Low losses of fast ions, arising during additional plasma heating and thermonuclear fusion reactions, are a necessary condition for steady-state operation of a thermonuclear reactor. The development of various magnetohydrodynamic (MHD) instabilities in plasma leads to losses and redistribution in the phase space of high-energy particles, which reduces plasma heating, current-drive and fusion performance, while increasing the thermal load on the in-vessel tokamak components. One type of instabilities that is dangerous to future thermonuclear facility are Alfvén-type instabilities [1], such as TAE – Toroidal Alfvén Eigenmode and EPM – Energetic Particle Mode. TAE (for the Globus-M/M2 characteristic instability frequency 100 kHz) exists in the continuous frequency spectrum gap, caused by the toroidicity of plasma and being weakly damped is easily destabilized by the super-alfvenic particles, while EPM (characteristic instability frequency 50 kHz) exists in continuum spectrum if the resonant drive from fast particles exceeds the threshold of the damping. Understanding

the mechanisms of Alfvén instability onset and their impact on heat loads is critical for developing strategies to control and mitigate their effects. The main transport mechanisms [2] are resonant transport and diffusion. Resonant transport is coherent with the wave and proportional to its amplitude, δB. Stochastic diffusion occurs when δB exceeds a certain threshold, scales as δB^2, and the resulting transport is incoherent with the mode.

At Globus-M/M2 spherical tokamaks (major radius R=0.36 cm and minor radius a=0.24 cm) the study of Alfvén modes were carried out in a wide range of plasma parameters: I_p = 160-450 kA, B_T = 0.4-0.9 T, $n_e = 10^{19}$-10^{20} m^{-3}, E_{NBI} = 20-50 keV, P_{NBI} = 0.3-1.5 MW. The non-dimensional parameter domain v_{fast}/v_a-$\beta_{fast}/\beta_{total}$ (where v_{fast} is velocity of the injected atoms, v_a is Alfvén velocity, β_{fast} is volume-averaged fast ion beta, β_{total} is the sum of the fast ion and plasma betas) of the experiments with TAEs at Globus-M/M2 covers domain of the future ITER DD and DT experiments (FIG. 1).

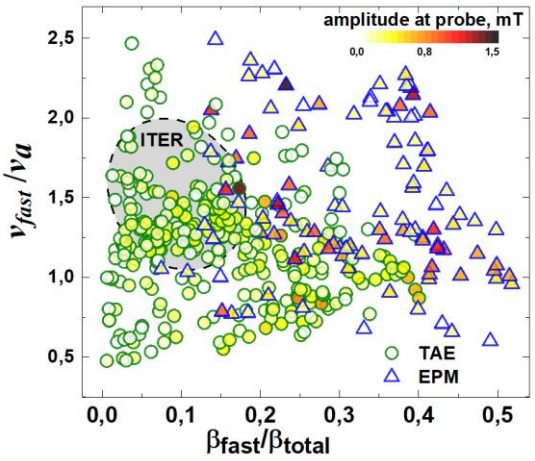

FIG.1. Alfvén-type instabilities parameter domain of the Globus-M/M2 experiments. Shaded regions—ITER parameter domain. The color differentiation of the dots corresponds to the amplitude of the burst.

2. DIAGNOSTIC SYSTEM DEVELOPMENT

A comprehensive investigation of wave-ion interaction processes requires the characterization of key elements: the plasma parameters, which define the Alfvén continuum properties; the wave properties, including frequency, mode structure, and spatial localization; the temporal evolution of the energetic ion distribution function, which is essential for identifying the dominant transport mechanism and assessing its potential consequences on the facility. An integrated multi-diagnostic approach [3] was used to address this problem:

— The ion temperature was measured by active spectroscopic diagnostics (CXRS). Electron temperature and density profiles were obtained from Thomson scattering (TS) diagnostics. The time evolution of the line-averaged density between TS measurements was provided by a microwave interferometer with a vertical chord at R = 42 cm. The effective charge, Z_{eff}, was determined based on measurements of plasma bremsstrahlung radiation intensity. The magnetic equilibrium was reconstructed using the EFIT code. A detailed description of the presented diagnostics can be found in [4];
— The characterization of Alfvén eigenmodes was performed using two sets of magnetic probes: a set of eight fast probes (50–300 kHz) uniformly distributed along the toroidal direction of the vacuum vessel, and a poloidal array of fifteen slow probes (0–150 kHz). The Doppler backscattering (DBS) method was used to localize the Alfvén eigenmodes [5];
— Two ACORD-type [6] neutral particle analyzers (NPAs), equipped with scanning systems and operating in active mode, were used to obtain the evolution of the fast ion spectrum with a temporal resolution of up to 0.1 ms. Tangential 16x16 silicon precision detector (SPD) [7] matrix array, with a high temporal resolution of 1.6 μs (enabling the observation of reactions to individual oscillations), was used to study co-going fast ion losses. In parallel, a single-channel SPD, with a resolution of ~0.2 ms (sufficient to resolve mode bursts), was employed to investigate losses of trapped and counter-going ions. Langmuir probe [8], installed at the equatorial plane, provided data on the ion saturation current, indicating the evolution of the ion flux near the separatrix. The neutron diagnostic system, based on boron counters in a polyethylene moderator (count rate

up to 100 kHz), was used as a primary indicator of fast ion confinement. A drop in the neutron rate or a slowdown of its growth was interpreted as a sign of either fast ion losses or their transport from the plasma core [9].

Over the past two years, tokamak diagnostic complex for fast particle studies has been significantly enhanced: an ITER-like U^{235} fission chamber was included (counting rate up to 2 MHz) [10], which improved neutron diagnostics temporal resolution by an order of magnitude. The development of fast ion plasma tomography was initiated by the installation of a fusion proton detector (counting rate up to 4 MHz) [11], also to study fast ion transport in a wider energy range a compact neutral particle analyzer (CNPA) [6] was installed. To study the tokamak's first wall heating due to high-energy particle losses during the interaction with Alfvén eigenmodes, an infrared camera (IR) [12] was installed, featuring a spatial resolution of ~1.3 mm/pixel and a temporal resolution of 0.3 ms for a 40×64 pixel frame and 4.5 ms for a 320×256 pixels frame. Studying the time evolution of fast particle losses to the tokamak wall became possible after installing a two-color pyrometer (time resolution up to 2 μs) [13].

The layout of the described diagnostics on the tokamak is shown in FIG. 2.

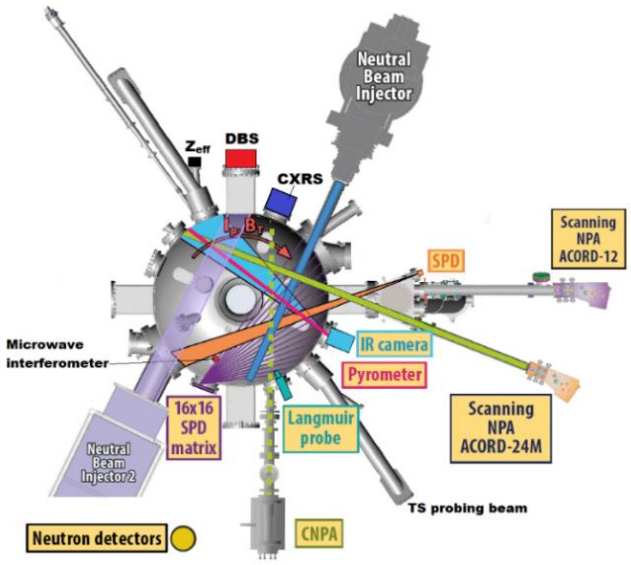

FIG. 2. Globus-M2 experimental layout (top view). Diagnostics marked with square boxes are used to directly study wave-induced fast ion losses and transport.

3. EXPERIMENTAL OBSERVATION OF THE FAST ION TRANSPORT AND LOSSES

The experiment investigated the evolution of the mode amplitude and frequency of a burst based on the fast magnetic probe signal [2]. A single down-chirping branch was observed. For this branch, the change in mode amplitude is consistent with linear theory, exhibiting exponential growth and decay. The frequency sweep is also described by an exponential function. These findings are consistent with the analytical model proposed by Berk and Breizman, when the anisotropy of the fast-ion distribution in Globus-M2 is considered [15,16].

Employing a multi-diagnostic approach, the interaction process between fast particles and TAE was studied [2]. Fast ion transport from the plasma center to the periphery was observed across a wide range of energies (FIG. 3). At the periphery, ions underwent charge exchange (CX) with neutral particles, whose density increases significantly near the last closed flux surface (LCFS), and were subsequently lost. These lost particles were detected by a fast SPD detector, which was employed to extract the coherent part of the loss signal correlated with the TAE activity. To identify the dominant transport mechanism governing the wave-particle interaction, the dependence of fast ion transport and losses on the TAE amplitude was studied in a series of dedicated experiments. A linear dependence without a threshold was identified for signal variations from various diagnostics. Only the signal from neutral particles at injection energy, measured by a NPA in active mode with a LOS towards the plasma periphery (8 degrees down from the equatorial plane), exhibited a linear dependence with a clear threshold.

Furthermore, these investigations revealed a significant reduction in fast ion transport with increasing value of I_p and B_t. This change in experimental conditions, and the associated decrease in energetic ion losses, led to a marked evolution in mode behaviour: instead of exhibiting individual bursts, continuously evolving TAEs developed.

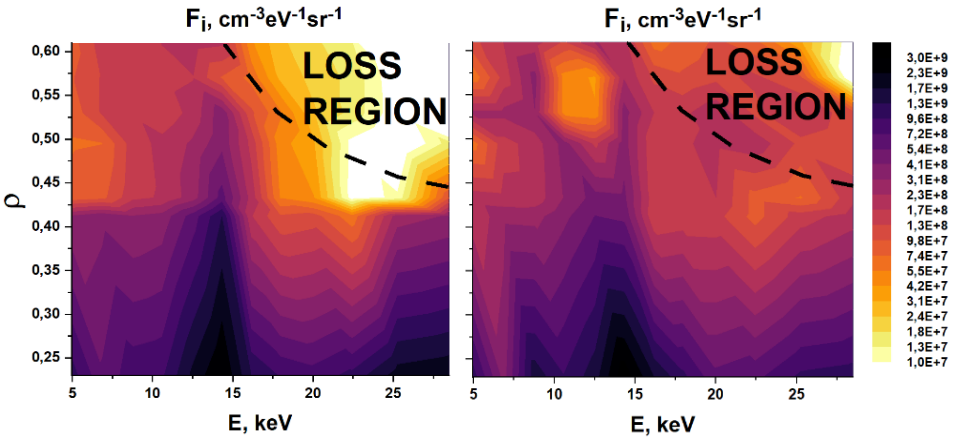

FIG. 3. Experimental energy and spatial fast D^+ distribution before (left) and during (right) TAE, reconstructed based on the active NPA measurements. Ion orbits behind the dashed black line intersect the LCFS.

Further studies were conducted using an IR-camera to monitor orbital losses from collisions with the tokamak wall during TAE instabilities [12]. Localized heating of the outer carbon tiles in the equatorial plane was measured, and the corresponding heat flux was calculated. A direct correlation was observed between intense TAE bursts and these localized temperature increases (FIG. 4 left), providing clear evidence of Alfvén wave-driven fast ion losse. The two-dimensional distribution of temperature changes on the carbon tiles during the TAE burst was measured (FIG. 4 right) and reveals non-uniform heating. Analysis confirms that most fast ions are lost to the wall primarily near the equatorial plane due to the minimal plasma-wall separation in that region. The non-uniform structure of the resulting heating profile is determined by a combination of inaccuracies in the manufacture of the first wall and the orbital trajectories of lost charged particles. Extending prior research, the flux of lost fast ions onto the wall was studied as a function of the instability amplitude, revealing a linear threshold dependence. Note that similar threshold-wise dependence was previously observed for atoms with injection energy recorded by the NPA with LOS towards the plasma periphery.

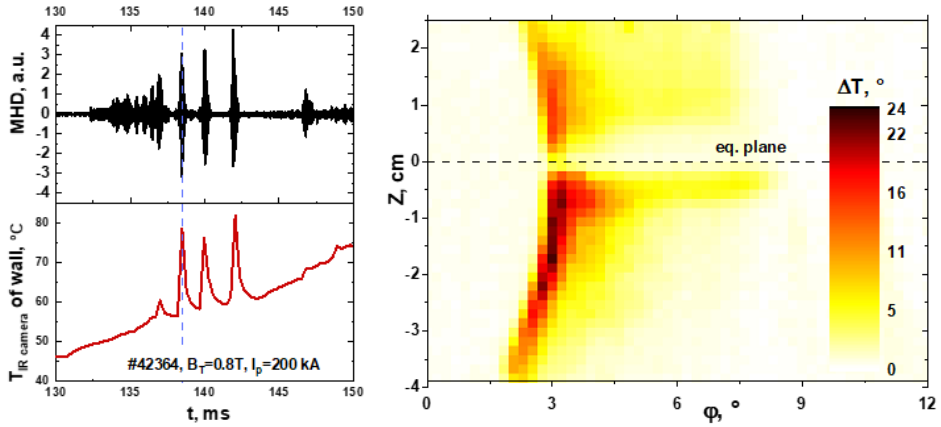

FIG. 4. (left) Time evolution of magnetic probe signal and carbon tile local temperature measured by IR camera. (right) Two-dimensional distribution of changes in carbon tiles temperature during burst of toroidal Alfven mode at the time indicated by the dashed line in the left figure. Z is vertical coordinate relative to equatorial plane and ϕ is toroidal angle. The dashed line marks the equatorial plane of the vacuum chamber.

Studies of fast particle losses and associated first-wall heating from wave-particle interactions were advanced by the installation of a two-color pyrometer on the tokamak. This diagnostic provides sufficient temporal resolution to directly measure the time evolution of fast ion losses during instability. Measurements were

performed locally (Ø 20 mm) on graphite plates in the equatorial plane of the vacuum chamber in the most heated region as measured by an infrared camera (see FIG. 4). Experimental measurements of the carbon tile temperature evolution during TAE burst are shown in FIG.5 (left). The figure also shows the evolution of the calculated local heat flux caused by fast ions hitting the wall. The incident fast particle flux can be separated into two components: "fast" coherent (relative to the magnetic probe signal) and "slow" incoherent. The growth of both components initiates simultaneously; however, their decay phases differ markedly. The coherent flux decays synchronously with the Alfvén mode, while the incoherent component decays much more slowly, with a characteristic decay time of $\tau_s \approx 0.6$ ms. The experiments also established the dependencies of both wall heating and heat flux on the mode amplitude (FIG.5 right). A linear threshold dependence was observed for the incoherent components (a behavior consistent with earlier infrared camera observations). The behavior of the coherent components is not described by a linear or quadratic function but can be approximated by two linear segments.

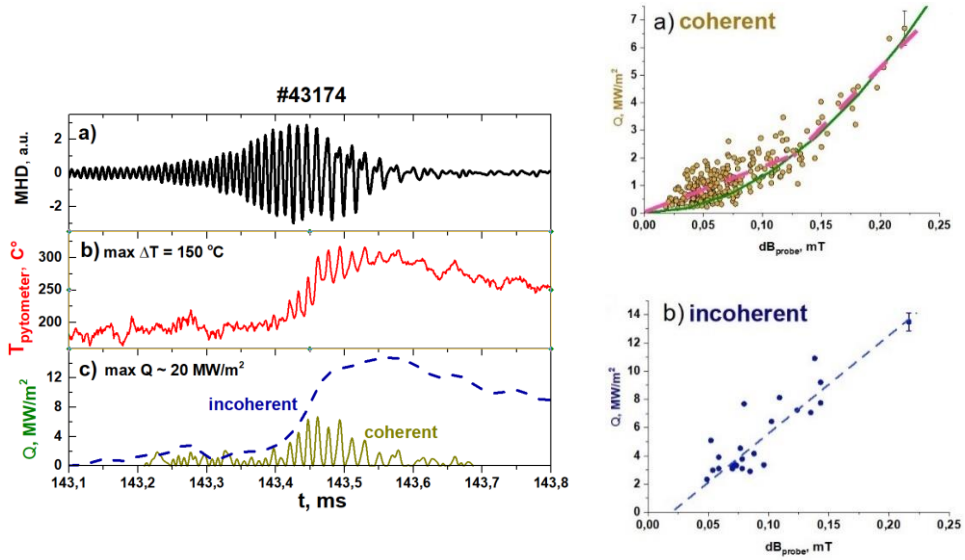

FIG.5. (left) Experimental measurement of wall heating during TAE burst in discharge #43174. From top to bottom: a) MHD probe signal, b) wall temperature measured by pyrometer, c) coherent (solid line) and incoherent (dashed line) heat flux for a film coefficient of 120 W $m^{-2}K^{-1}$. An increase in local wall temperature to 150 °C was experimentally observed, which corresponded to a local heat flux of up to ~20 MW/m^2. (right) Dependence of the coherent (a) and incoherent (b) components of the time evolution of the heat flux to the wall on the amplitude of the TAE measured by a magnetic probe. The solid line shows the quadratic dependence, and the dashed line shows the approximation of the experimental points by two linear dependences.

4. SIMULATION AND RESULTS

To explain the experimental observations, a simplified Monte Carlo simulation was developed to investigate TAE-induced fast ion losses and redistribution in phase space. The general approach introduced in [2] was used as a basis but was modified to accurately capture the conditions of a small spherical tokamak with high ρ_L/a (where ρ_L – Larmor radius, a - minor radius). First, an anisotropic fast ion distribution function, pre-calculated using the NUBEAM code prior to the TAE burst, was used instead of an isotropic one. Second, the full-orbit approach was employed instead of the guiding center approximation, as the size of the energetic ion Larmor radius is comparable to the mode width. During the simulation, taking into account the calculated distribution function, an ensemble of 10^5 ions was generated. Each ion was monitored for 0.1-0.4 ms (depending on the task) in time-varying three-dimensional magnetic and electric fields to identify particles undergoing losses. For simplicity, a particle was considered lost if its orbit intersected the LCFS, an assumption validated in MHD-quiescent discharges and justified by the fact that the charge exchange time near the plasma edge is much shorter than the slowing-down time in the Globus-M/M2 tokamaks. The mode characteristics – frequency, localization, amplitude, toroidal (n) and poloidal (m) mode numbers – were taken from direct experimental measurements (DBS and magnetic probes), and the linear phase of the mode was calculated. Note that the three-dimensional structure of

the tokamak wall was not included in the model; consequently, the simulation could only calculate the total fast-ion loss load integrated over the toroidal wall. It should also be noted that the simulation assumed a constant mode frequency, thus neglecting the temporal evolution of the TAE burst.

To explain the experimentally observed transport of fast particles across a wide energy range (FIG. 3), this modeling was employed [3]. FIG. 6 demonstrates the calculated dependence of the maximum ion orbit shift on energy and normalized effective radius during a TAE burst with different frequencies, obtained from a vertical NPA scan. The value at each point represents the maximum displacement of an ion orbit from a set of ions tracked over 100 mks of wave-particle interaction. This set included ions with initial toroidal angles from 0 to 2π to account for all possible relative phases between the wave and the particles. As can be seen from the figure, the numerical results predict a broad resonance area. Thus, the simulations confirm that ion transport occurs across a wide energy range, with ions above ~15 keV undergoing the most significant spatial redistribution.

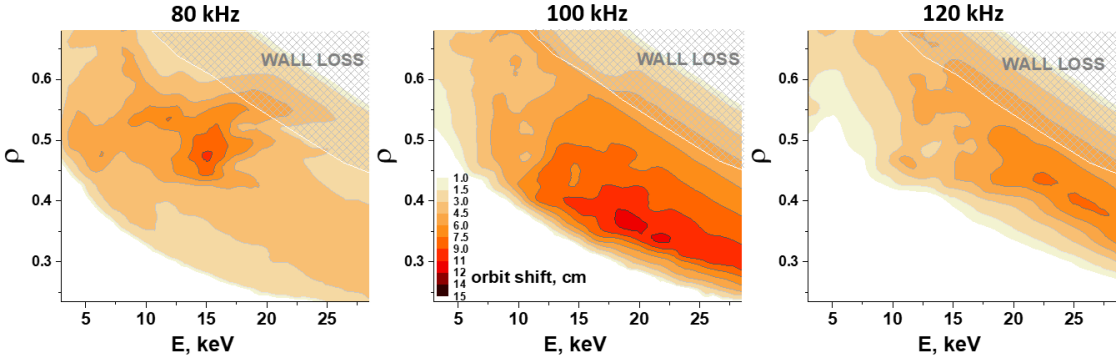

FIG.6. Estimated dependence of the maximum ion orbit shift on energy and normalized effective radius during 0.1 ms TAE bursts at frequencies of 80 kHz (left), 100 kHz (center), and 120 kHz (right) at vertical NPA scan. The shaded area denotes the region of first-orbit losses due to wall collisions.

Simulations of the fast ion loss fraction and loss rate dependence on TAE amplitude were also performed. The simulation results are consistent with experimental observations: despite the unique features of Globus-M/M2, the results show that losses scale linearly with wave amplitude, and no significant diffusion occurs at experimentally observed amplitudes. The temporal structure of losses showed periodicity equal to the TAE cycle, indicating a coherent, non-diffusive mechanism.

This modeling approach was also used to simulate fast ion losses during wave interactions to calculate the resulting heat flux onto the tokamak first wall. The results reproduce key experimental observations: predominant heat deposition on the outer wall near the midplane with stronger heating below the equator, and a sharp threshold-like increase in heat load at wave amplitudes exceeding ~0.2 mT (close to the experimentally observed threshold). The conducted modelling successfully explains the observed threshold dependence. The simulations demonstrate that low-amplitude instabilities can only eject ions from the plasma periphery, where their concentration is low due to high charge-exchange losses, resulting in negligible heating of the carbon tiles. However, once the instability amplitude exceeds a critical threshold, it becomes sufficient to transport ions from the plasma core – where their concentration is orders of magnitude higher. This transition causes an abrupt increase in the wall heat load, which manifests experimentally as a distinct threshold in the amplitude dependence. Thus, the observed threshold behaviour is not caused by diffusion but is directly linked to the characteristic spatial distribution of fast ions at Globus-M2. Also, the modeling explains the correlation between the threshold behavior from the infrared camera signal and peripheral active NPA measurements. Trajectory simulations show that ions detected by the inclined NPA after CX in the target region have orbits intersecting the tokamak wall, confirming that both diagnostics monitor the same population of lost fast ions: while the infrared camera measures localized wall heating from particle impacts, the NPA signal is proportional to the density of these particles just before their loss.

Furthering the investigation, we now consider the measurements from the two-colour pyrometer (FIG.5): the extracted coherent heat flux component is likely determined by a convective transport mechanism. In contrast, the temporal evolution of the incoherent heat flux – a rise throughout the burst followed by a slow decay – cannot be directly explained by the considered mechanisms. We hypothesize that this component is linked to charge-exchange losses of fast ions, as the decay time of the incoherent flux (~1 ms) is comparable to the characteristic CX time near the plasma boundary – a primary loss channel in quiescent Globus-M2 plasmas. The proposed

mechanism is that wave-particle interaction shifts ion orbits closer to the plasma boundary. While most shifted orbits still do not intersect the wall, the sharply increased neutral density there enhances the probability of charge exchange. Consequently, the additional heat flux arises not from direct fast ion losses, but from fast atoms generated near the wall.

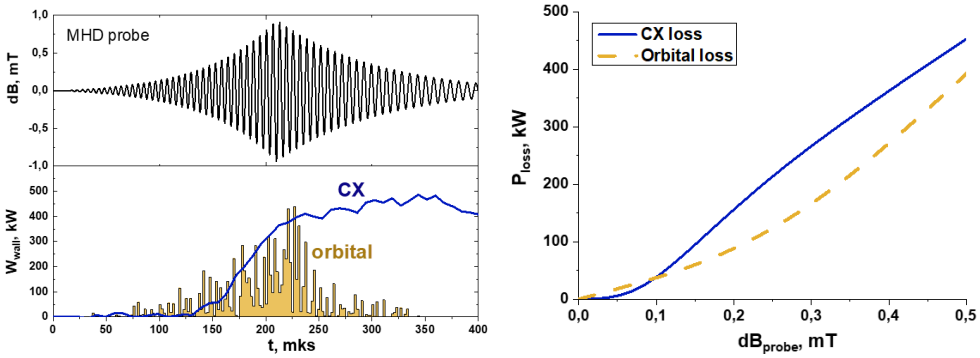

FIG.7. (left) Simulation of fast-ion losses during the development of a TAE. Top to bottom: magnetic field oscillations at the probe location; fast-ion losses: histogram – due to orbit intersection with the wall, solid line – due to charge exchange. (right) Calculated dependence of the loss power due to wall collisions (dashed line) and charge exchange (solid line) on the amplitude of the Alfvén mode.

To test this hypothesis, simulations using the previously described approach were performed. FIG.7 (left) shows the temporal evolution of orbital losses due to direct wall impact and charge-exchange losses within a narrow toroidal angle region, normalized to the total loss value. The simulated heat flux exhibits both coherent and incoherent components, matching experimental observations. The coherent component scaled with magnetic fluctuation amplitude, while the incoherent component showed continuous growth during the burst, where significant amplification commenced at a threshold magnetic fluctuation amplitude and ceased with the instability's fading. The simulations confirmed the coherent flux originated from direct fast ion wall impacts, while the incoherent component, as hypothesized, was dominated by CX losses near the plasma boundary. It is noteworthy that orbital losses also exhibit a small incoherent component attributable to the finite time (≤ one poloidal rotation period, comparable to the instability period) required for an ion on a loss orbit to reach the wall. The simulations also enabled calculation of the dependence of the loss power for the coherent and incoherent components on the instability amplitude (FIG.7 right). The resulting dependence of the incoherent heat flux, originating from CX atoms, on the mode amplitude exhibits a clear threshold behaviour. This dependence, however, is not attributable to a diffusive transport mechanism, as already noted, but rather to the specific redistribution of fast ions into regions of phase space where CX losses are predominant. For the coherent component, a linear dependence with an inflection point is observed. A comparison with experimental data (FIG. 5) reveals that the simulated inflection amplitude is approximately a factor of two greater than the measured value, which is likely attributable to model limitations.

In summary, the performed calculations and experimental data analysis demonstrate that both fast-ion loss mechanisms – orbital and charge-exchange – are caused by the convective resonance mechanism of fast ion transport from the plasma center to the periphery.

5. INITIAL INVESTIGATION OF ENERGETIC PARTICLE MODES (EPMS)

The enhancement of plasma parameters and fast-ion confinement in the Globus-M2 tokamak led to the emergence of previously unobserved Energetic Particle Modes (EPMs). As shown in FIG.1, these instabilities populate the upper-right region of the non-dimensional parameter domain v_{fast}/v_a-$\beta_{fast}/\beta_{total}$, contrasting with TAEs that primarily occupy the lower-left region. Notably, EPMs were observed even in discharges with strong sawtooth oscillations.

For the first time at Globus-M2, a direct correlation between EPM-induced fast ion transport and losses was experimentally measured (FIG. 8). Firstly, a clear decrease in the flux of charge-exchange atoms with an energy of 28.5 ± 1.2 keV was recorded by an active NPA with a line of sight (LOS) in the equatorial plane (FIG. 8, left); this reduction signifies the redistribution of fast ions from the core plasma. Secondly, a synchronous

increase in the temperature of the graphite first wall tiles was detected by a pyrometer (FIG. 8, right), providing direct evidence of the loss of these fast ions and their energy deposition on the plasma-facing components.

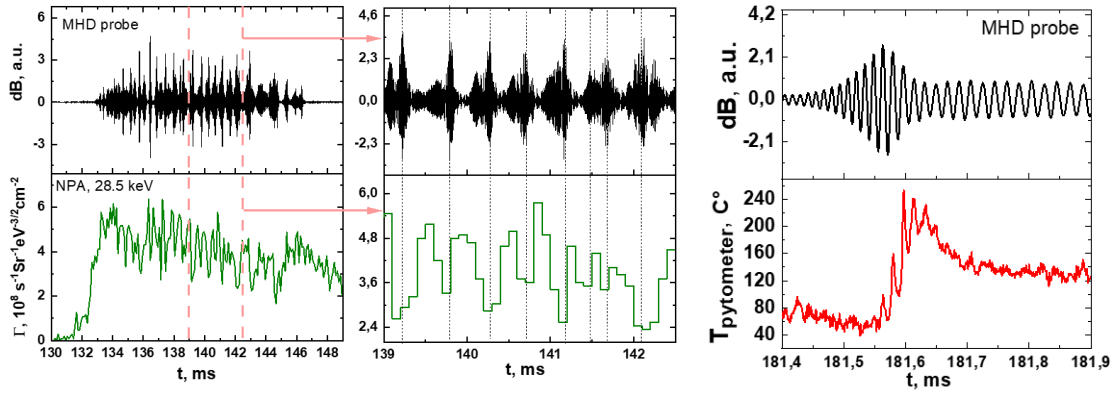

FIG.8. (left) Experimental observation of the EPMs-induced transport and losses. From top to bottom: magnetic probe signal, variation of the 28.5±1.2 keV atom count rate, obtained with active NPA measurements with LOS in the equatorial plane (central ion transport study). The dashed lines mark a segment that is displayed with expanded temporal resolution in the middle panel. (right) Experimental measurement of wall heating during EPMs burst in discharge #42411. From top to bottom: MHD probe signal, wall temperature measured by pyrometer.

ACKNOWLEDGEMENTS

Works were carried out on the Unique Scientific Facility "Spherical tokamak Globus-M", which is incorporated in the Federal Joint Research Center "Material science and characterization in advanced technology". The studies of fast ions were supported by the Russian Science Foundation (project no. 21-72-20007-P)

REFERENCES

[1] W.W. Heidbrink, Phys. Plasma 15, 055501 (2008)
[2] D. J. Sigmar, C. T. Hsu, R. White, and C. Z. Cheng, Phys. Fluids B 4, 1506 (1992).
[3] N.N. Bakharev, et al. Phys. Plasmas 30, 072507 (2023)
[4] Yu. V. Petrov, et al. Plasma Phys. Rep., 49, 1459 (2023)
[5] V.V. Bulanin, et al. Tech. Phys. Lett. **47**, 197 (2021)
[6] N.N. Bakharev, et al. Atoms 11, 53 (2023)
[7] A.P. Artyomov, et al. Instrum. Exp. Tech. 58, 102 (2015)
[8] V.A. Tokarev, et al. J. Phys.: Conf. Ser. 1094, 012003 (2018)
[9] M.V. Iliasova, et al. NIM A 1029, 166425 (2022)
[10] I.N. Aristov, et al. Inst. and Exper. Tech. 47, 147–152 (2004)
[11] N.N. Bakharev, et al. Tech. Phys. Lett. 50, 24, (2024)
[12] N.N. Bakharev, et al. Plasma Phys. Rep. 49, 1524-1532 (2023)
[13] N.N. Bakharev, et al. Plasma Phys. Rep. - accepted manuscript.
[14] J. Zhu, Z. W. Ma, and G. Y. Fu, Nucl. Fusion 54, 123020 (2014)
[15] R. G. L. Vann, R. O. Dend, and M. P. Gryaznevichet, Phys. Plasmas 12, 032501 (2005)